Protein Coingestion with Alcohol Following Strenuous Exercise Attenuates Alcohol-Induced Intramyocellular Apoptosis and Inhibition of Autophagy

William J. Smiles[1], Evelyn B. Parr[1], Vernon G. Coffey[2], Orly Lacham-Kaplan[1], John A. Hawley[1, 3] and Donny M. Camera[1]

[1]Mary MacKillop Institute for Health Research, Centre for Exercise and Nutrition, Australian Catholic University, Melbourne, Victoria, Australia; [2]Bond Institute of Health and Sport and Faculty of Health Sciences and Medicine, Bond University, Queensland, Australia; [3]Research Institute for Sport and Exercise Sciences, Liverpool John Moores University, Liverpool, United Kingdom

Running Title: Alcohol, exercise and muscle homeostasis

Author Contributions: WJS, EBP, VGC, JAH and DMC designed the research. WJS, EBP, VGC, and DMC conducted the research. WJS, OLK and DMC analysed the data and/or performed statistical analysis. WJS, VGC, OLK, JAH and DMC wrote the paper. WJS, OLK, JAH and DMC had primary responsibility for its final content.

Author for correspondence:
Donny Camera
Mary MacKillop Institute for Health Research
Centre for Exercise and Nutrition Australian Catholic University
Fitzroy VIC 3165
Australia
Email: donny.camera@acu.edu.au
Phone: +61 3 9953 3527
Fax: +61 3 9953 3095

ABSTRACT

Alcohol ingestion decreases post-exercise rates of muscle protein synthesis, but the mechanism(s) (e.g., increased protein breakdown) underlying this observation are unknown. Autophagy is an intracellular "recycling" system required for homeostatic substrate and organelle turnover; its dysregulation may provoke apoptosis and lead to muscle atrophy. We investigated the acute effects of alcohol ingestion on autophagic cell signaling responses to a bout of concurrent (combined resistance- and endurance-based) exercise. In a randomized cross-over design, 8 physically active males completed three experimental trials of concurrent exercise with either post-exercise ingestion of alcohol and carbohydrate (12±2 standard drinks; ALC-CHO), energy-matched alcohol and protein (ALC-PRO), or protein (PRO) only. Muscle biopsies were taken at rest and 2 and 8 h post-exercise. Select autophagy-related gene (Atg) proteins decreased compared to rest with ALC-CHO (P<0.05), but not ALC-PRO. There were parallel increases (P<0.05) in p62 and PINK1, commensurate with a reduction in BNIP3 content, indicating a diminished capacity for mitochondria-specific autophagy (mitophagy) when alcohol and carbohydrate were coingested. DNA fragmentation increased in both alcohol conditions (P<0.05); however, nuclear AIF accumulation preceded this apoptotic response with ALC-CHO only (P<0.05). In contrast, increases in the nuclear content of p53, TFEB and PGC-1α in ALC-PRO were accompanied by markers of mitochondrial biogenesis at the transcriptional (*Tfam*, *SCO2*, *NRF-1*) and translational (COXIV, ATPAF1, VDAC1) level (P<0.05). We conclude that alcohol ingestion following exercise triggers apoptosis, whereas the anabolic properties of protein coingestion may stimulate mitochondrial biogenesis to protect cellular homeostasis.

Keywords: Alcohol, exercise, autophagy, apoptosis, protein

INTRODUCTION

Exercise sensitizes skeletal muscle to exogenous nutrient availability, such that substrate availability interacts with cellular processes regulating protein turnover responses that ultimately form the basis for exercise adaptation (20). While the carbohydrate and protein requirements to promote adaptation to divergent exercise stimuli (i.e., endurance- and resistance-based) are well-characterized (8, 44), far less is known regarding the impact of alcohol ingestion on exercise response-adaptation processes. Given the widely reported alcoholic drinking practices of professional and recreational athletes (9), and the capacity for "binge" alcohol consumption to impair recovery-performance and muscle protein synthesis (MPS) rates following strenuous exercise (5, 41), elucidating the mechanisms that underpin these detrimental effects of exercised skeletal muscle exposed to alcohol is warranted.

Previous studies in rodents report that large quantities of alcohol dysregulate the stimulation of MPS by growth factors and amino acids, largely due to attenuated signal transduction of the mammalian target of rapamycin (mTOR) complex 1 pathway (30, 31), a principal modulator of cellular growth. Similarly, alcohol was found to reduce the maximal MPS response to high-force mechanical overload in rodents (56, 57). Recently, we showed that alcohol ingested following a single bout of strenuous exercise attenuated the maximal exercise- and nutrition-induced stimulation of the myofibrillar (contractile) fraction of protein synthesis, despite exogenous protein availability (41). While the capacity for alcohol to impair MPS is recognized, its impact upon intramuscular protein degradative pathways is less clear. Acute alcohol exposure had no effect on proteasome-dependent proteolysis in rodents (62) and we found no synergistic effect of alcohol toward the transcription of key proteasome-related ubiquitin ligases following exercise (41). Whether autophagy, the constitutive turnover of cellular components such as long-lived organelles (e.g.,

mitochondria) that protects homeostasis and is required for skeletal muscle integrity (24), promotes skeletal muscle catabolism in response to alcohol ingested following an acute exercise bout, is unknown.

Alcohol metabolism produces highly-toxic intermediates that may accelerate cellular metabolism and exacerbate tissue breakdown responses to vigorous contractile activity (33). Furthermore, autophagy is sensitive to the cellular energetic balance and "recycles" nutrient substrate and organelles to maintain cellular viability (52). Thus, a post-exercise autophagic response to alcohol may represent a compensatory removal of harmful protein aggregates that can trigger cell death processes (apoptosis) (1). Accordingly, the primary aim of this study was to investigate the activation of autophagic cell signaling responses to binge alcohol consumption during recovery from a single bout of combined resistance and endurance ("concurrent") exercise. Due to the anabolic properties of amino acids and their capacity to inhibit autophagic flux (39), we hypothesized that the largest autophagic response would occur when alcohol and carbohydrate were coingested compared to protein following exercise. We also hypothesized that alcohol would elicit an increased mitophagic (mitochondria-selective autophagy) cell signaling response, since the catabolism of alcohol metabolites predominates in the mitochondria and is a source of reactive oxygen species (ROS) production, which may stimulate mitophagy and provoke muscle protein breakdown responses (47, 61).

MATERIALS AND METHODS

Subjects

Eight young, healthy, physically active male subjects [age 21.4 ± 4.8 yr, body mass (BM) 79.3 ± 11.9 kg, were recruited from a previous study (41). Full subject characteristics, preliminary testing procedures (VO_{2peak} and maximal muscular strength), diet and exercise control, and complete details of the experimental design and experimental trials have been reported (41). Due to the legal drinking age in Australia, no minors (<18 yr old) were involved in the study. Subjects were advised of any possible risks associated with the study prior to providing written informed consent. The study was approved by the Human Research Ethics Committee of RMIT University (43/11) and was carried out in accordance with the standards set by the latest revision of the *Declaration of Helsinki*.

Experimental Design

The study employed a randomized, counter-balanced crossover design in which each subject completed, on three separate occasions, trials consisting of a bout of concurrent exercise (described subsequently) with either post-exercise ingestion of alcohol and carbohydrate (ALC-CHO), alcohol and protein (ALC-PRO) or protein only (PRO), in which carbohydrate and protein beverages were consumed twice; before and after the alcohol drinking protocol. Each experimental trial was separated by a two week recovery period, during which time subjects resumed their habitual pattern of physical activity.

Experimental Trials

Subjects reported to the laboratory at ~0700 h on the morning of an experimental trial following a 10 h overnight fast and a resting muscle biopsy was taken from the *vastus lateralis* under local anaesthesia (1% lidocaine) using a 5 mm Bergstrom needle modified for

suction. Subjects then commenced the concurrent exercise bout which consisted of heavy resistance exercise (8 × 5 knee extension repetitions at 80% of 1 repetition maximum), followed by 30 min of cycling at ~70% of VO_{2peak}, and then a high-intensity (10 × 30 s, 110% PPO) interval cycling bout. Immediately post-exercise and following 4 h of recovery, subjects ingested 500 mL of a carbohydrate (CHO: 25 g maltodextrin) or an isoenergetic protein (PRO: 25 g whey) beverage. Consistent with recommendations for CHO feeding and glycogen resynthesis following training (8), an additional CHO-based meal (1.5 $g \cdot kg^{-1}$ BM) was provided immediately after the first post-exercise (2 h) muscle biopsy with a final muscle biopsy obtained 8 h post-exercise. Muscle biopsies were taken from separate incision sites, cleared of visible adipose and/or connective tissue, snap-frozen in liquid nitrogen and stored at −80 ˚C for subsequent analysis. Subjects commenced drinking alcohol 1 h post-exercise and drinks were consumed in 6 equal volumes of 1 part vodka (~60 mL) to 4 parts orange juice (~240 mL, 1.8 g $CHO \cdot kg^{-1}$ BM) across a 3 h period (12 ± 2 standard drinks consumed), in which alcoholic beverages were consumed within 5 min every 30 min. For PRO trials, subjects still consumed orange juice with a matched volume of water (Fig. 1).

Analytical Procedures

Skeletal Muscle Sample Preparation

For generation of whole muscle lysates, ~40 mg of skeletal muscle was homogenized in buffer containing 50 mM Tris·HCl, pH 7.5, 1 mM EDTA, 1 mM EGTA, 10% glycerol, 1% Triton X-100, 50 mM NaF, 5 mM sodium pyrophosphate, 1 mM DTT, 10 μg/mL trypsin inhibitor, 2 μg/mL aprotinin, 1 mM benzamidine and 1 mM PMSF. Samples were spun at 16,000 *g* for 30 min at 4 ºC and the supernatant was collected for Western blot analysis. Nuclear and cytoplasmic extracts were prepared using an NE-PER fractionation kit according to the manufacturer's instructions (Thermo Scientific, Rockford, IL). In brief, ~30 mg of

158 skeletal muscle was homogenized on ice, by hand, using a glass Dounce homogenizer in
159 CER-I (cytoplasmic extraction reagent-I) buffer supplemented with protease and phosphatase
160 inhibitors. Homogenized samples were vortexed and incubated on ice for 10 min, after which
161 the CER-II buffer was added. CER-II-containing samples were vortexed and subsequently
162 spun at 16,000 *g* for 5 min at 4 ºC with the supernatants containing cytoplasmic proteins
163 removed and the remaining nuclei-containing pellet resuspended in nuclear extraction reagent
164 buffer (supplemented with inhibitors). Nuclear lysates were subsequently incubated on ice
165 and vortexed for 15 s every 10 min for a total of 40 min, with a final 10 min centrifugation
166 (16,000 *g* at 4 ºC) for collection of nuclear supernatants.
167
168 *Western Blotting*
169 After determination of protein concentration using a BCA protein assay (Pierce, Rockford,
170 USA), all lysates (50 μg and 10 μg of protein for whole muscle and fractionated lysates,
171 respectively) were resuspended in Laemmli sample buffer and loaded into 4–20% Mini-
172 PROTEAN TGX Stain-Free™ Gels (Bio-Rad, California, USA). Following electrophoresis,
173 gels were activated according to the manufacturer's instructions (Chemidoc, Bio-Rad,
174 Gladesville, Australia) and transferred to polyvinylidine fluoride (PVDF) membranes as
175 performed previously (55). After transfer, a Stain-Free image of the PVDF membranes for
176 total protein normalization was obtained before membranes were rinsed briefly in distilled
177 water and blocked for 1 h with 5% non-fat milk, washed 3 times (5 min each wash) with 10
178 mM Tris·HCl, 100 mM NaCl and 0.02% Tween 20 (TBST) and incubated with a primary
179 antibody diluted in TBST (1:1,000) overnight at 4 °C on a shaker. Membranes were
180 incubated for 1 h the next day with a secondary antibody diluted in TBST (1:2,000) and
181 proteins were detected via enhanced chemiluminescence (Amersham Biosciences,
182 Buckinghamshire, UK; Pierce Biotechnology) and quantified by densitometry (Chemidoc,

BioRad, Gladesville, Australia). All sample time points for each subject were run singularly on the same gel. Antibodies against phospho-ULK1 Ser^{317} and Ser^{757} (no. 12753 and no. 6888, respectively), Atg4b (no. 5299), Atg5 (no. 2630), cAtg12 (no. 4180), Beclin-1 (no. 3738), LC3b (no. 2775), p62 (no. 5114), NEDD4 (no. 2740), PINK1 (no. 6946), Parkin (no. 2132), BNIP3 (no. 44060), AIF (no. 5318), PARP1 (no. 9542), caspase-3 (no. 9662), TFEB (no. 4240), phospho-AMPK^{Thr172} (no. 2531), AMPKα (no. 2532), phospho-p53^{Ser15} (no. 9284), p53 (no. 2527), COXIV (no. 4850), Mitofusin-2 (no. 11925), H2B (no. 8135) and GAPDH (no. 2118) were purchased from Cell Signaling Technology (Danvers, MA). Antibodies directed against PGC-1α (ab54481), ATPAF1 (ab101518), VDAC1 (ab14734) and an additional LC3b antibody (ab48394) were purchased from Abcam (Melbourne, Australia). For all proteins, volume density of each target band was normalized to the total protein loaded into each lane (Fig. 2*A*) using Stain-Free™ technology (Bio-Rad, California, USA) (18, 55). Purity of the cytoplasmic and nuclear fractions was determined by immunoblotting for the glycolytic enzyme GAPDH and the nuclear histone 2B, respectively (Fig. 2*B*). Due to limited tissue size, analysis of fractionated samples was restricted for some time points: For the majority of proteins measured, ALC-CHO 2 h (n=7), ALC-PRO 2 h (n=6) and 8 h (n=7), and PRO 2 h (n=6) and 8 h (n=7) time points were restricted. There was n=5 for some time points of Parkin (ALC-PRO 2 h, PRO 8 h), PARP1 (ALC-PRO 2 h, PRO 2 h), phospho-AMPK^{Thr172} and ATPAF1 (both PRO 8 h). Due to difficulties in quantification (non-specific binding), cytoplasmic p53 analysis was also based on n=5.

RNA Extraction, Quantification, Reverse Transcription and Real-Time PCR

Skeletal muscle tissue RNA extraction was performed using a TRIzol-based kit according to the manufacturer's protocol (Invitrogen, Melbourne, Australia, Cat. No. 12183–018A). Briefly, ~20 mg of frozen skeletal muscle tissue was homogenized in TRIzol with chloroform

added to form an aqueous RNA phase. This RNA phase was then eluted through a spin cartridge with extracted RNA quantified using a NanoDrop 2000 Spectrophotometer (Thermo Scientific, Scoresby, Australia) according to the manufacturer's protocol. Reverse transcription and real-time Polymerase Chain Reaction (RT-PCR) was performed as previously described (55). Quantification of mRNA in duplicate was performed using a CFX96 Touch™ Real-Time PCR Detection System (Bio Rad, California, USA). TaqMan-FAM-labelled primer/probes for *Atg12* (Hs01047860), *BECN1* (Hs00186838), *LC3b* (Hs00797944), *SQSTM1*/*p62* (Hs01061917), *Atg4b* (Hs00367088), *BNIP3* (Hs00969291), *SCO2* (Hs04187025), *SESN-2* (Hs00230241), *PUMA* (Hs00248075), *Bax* (Hs00180269), *PGC-1α* (Hs01016719), *Tfam* (Hs00273372) and *NRF-1* (Hs01031046) were used. *GAPDH* (Hs99999905) has been validated as an exercise housekeeping gene (23) and was used to normalize threshold cycle (CT) values. *GAPDH* values were stably expressed between conditions (data not shown). The relative amount of mRNA was calculated using the relative quantification (ΔΔCT) method (35).

Cell Death ELISA

Detection of DNA damage and cell death (apoptosis) was performed using a cell death detection ELISA (Roche Diagnostics, Mannheim, Germany). The cell death ELISA quantitatively determines apoptotic DNA fragmentation by measuring the cytoplasmic histone-associated mono- and oligonucleosomes. Briefly, even concentrations (120 µg) of nuclei-free cytoplasmic lysates were loaded as an antigen source to an anti-histone monoclonal antibody fixated to the walls of microplate modules. Lysates were loaded prior to the addition of an anti-DNA secondary antibody conjugated to peroxidase. The amount of peroxidase retained in the immunocomplex was determined photometrically by incubating with 2,2′-azino-di-[3-ethylbenzthiazoline sulphonate] (ABTS) as a substrate on a plate shaker

(300 rpm) for ~15 min at room temperature (20 ºC). Absorbance was measured at a wavelength of 405 nm using a SpectraMax Paradigm plate reader (Molecular Devices, Sunnyvale, CA, USA). Samples were measured in duplicate on the same plate and absorbance values were normalized to µg of protein loaded in the assay per sample. Due to limited cytoplasmic lysate availability sample analysis was restricted for ALC-CHO 2 h (*n*=7), ALC PRO 2 h (*n*=6), ALC PRO 8 h (*n*=7), PRO 2 h (*n*=5) and PRO 8 h (*n*=6).

GSH/GSSG Ratio

Detection of oxidative stress was performed using a GSH/GSSG Ratio Detection Assay Kit (Abcam, Melbourne, Australia). Cytoplasmic lysates were first deproteinized by adding trichloroacetic acid (TCA) to the samples in a 1:10 dilution. Samples were then incubated on ice (15 min) and briefly centrifuged (5 min, 12,000 *g* at 4 ºC) with the supernatant removed and neutralized of excess TCA using a neutralizing solution (Abcam, Melbourne, Australia). The assay was performed using standards for reduced (GSH) and oxidized (GSSG) glutathione. Samples (*n*=4) were incubated for ~45 min at room temperature (20 ºC) in a Thiol Green Stock solution diluted in assay buffer (GAM) and a 25X GSSG Probe diluted in GAM solution for the detection of reduced and oxidized glutathione, respectively. Fluorescence was measured at an excitation/emission wavelength of 490/520 nm using a SpectraMax Paradigm plate reader (Molecular Devices, Sunnyvale, CA, USA). Samples were measured in duplicate on the same plate and fluorescence values were normalized to µg of protein loaded in the assay per sample.

Statistical Analysis

Data were analyzed using two-way repeated measures analysis of variance (ANOVA) with Student-Newman-Keuls post-hoc analysis (time × treatment) performed when an overall

statistically significant difference in group means of a particular comparison was found (SigmaPlot for Windows; Version 12.5). Significance was set to $P<0.05$ and all data are presented as mean ± standard deviation (SD). When tests for normality and/or equal variance failed, data were log-transformed and statistical inferences were made based on these data.

RESULTS

Autophagy Regulatory Proteins

Autophagy involves the formation of vesicles termed autophagosomes that sequester and deliver cellular constituents to lysosomes for degradation in a process regulated by autophagy-related gene (Atg) proteins (38). AMP-activated protein kinase (AMPK)-targeted phosphorylation of Atg1 or unc-51-like kinase 1 (ULK1) at Ser^{317} that activates autophagy was unchanged with any exercise-nutrient stimulus (data not shown). In contrast, $ULK1^{Ser757}$ phosphorylation, a site targeted by mTOR that inhibits autophagy induction (28), increased ($P<0.05$) with PRO above rest and each alcohol treatment (data not shown). Whole muscle abundance of Atg4b, Atg5, the conjugated form of Atg5 (cAtg12) and Beclin-1 all decreased compared to rest at 8 h post-exercise in ALC-CHO only ($P<0.05$; Fig. 3*A*-*D*), while Atg5 and cAtg12 values at 8 h post-exercise were greater in ALC-PRO than ALC-CHO ($P<0.05$). All Atg proteins except Beclin-1 were higher than ALC-CHO in PRO at 8 h post-exercise ($P<0.05$). An indirect marker of autophagosome formation is an increase in the lipidated membrane-bound form of light chain 3b (LC3b-II) and a decrease in p62 (59). There were no differences in the non-lipidated LC3b-I isoform with any exercise-nutrient condition (Fig. 3*E*), although LC3b-II decreased below rest at 2 h ($P<0.05$) and remained attenuated by 8 h post-exercise in ALC-CHO ($P=0.052$; Fig. *3F*). LC3b-II similarly decreased below rest at 8 h with PRO ($P<0.05$). p62 increased above rest at 8 h post-exercise in ALC-CHO ($P<0.01$; Fig. 3*G*), while similar increases also occurred between 2-8 h of exercise recovery in ALC-PRO

283 (P<0.05). These findings altogether suggest that alcohol coingested with carbohydrate, but
284 not protein, inhibited autophagy. To gain insight into whether this inhibition culminated from
285 elevated Atg degradation by the proteasome, we measured the ubiquitin ligase neural
286 precursor cell expressed developmentally downregulated 4 (NEDD4), which has been shown
287 to target Beclin-1 for proteasomal degradation (45). However, NEDD4 declined below rest at
288 8 h post-exercise with ALC-CHO only (P<0.05; Fig. 3*H*), suggesting that the alcohol-
289 induced reduction in Atgs was probably not attributable to their proteasomal breakdown.
290
291 *Autophagy Regulatory Genes*
292 There were no changes in the mRNA transcripts of *Atg12*, *BECN1*, *LC3b* and *SQSTM1*/*p62*.
293 However, *Atg4b* increased (P<0.05) above rest at 8 h following exercise in both alcohol
294 treatments (data not shown).
295
296 *Mitochondria-Specific Autophagy (Mitophagy)*
297 PTEN-induced putative protein kinase-1 (PINK1) and Parkin regulate canonical mitophagy.
298 There were large increases in PINK1 above rest for ALC-CHO and PRO at 8 h post-exercise
299 (P<0.01; Fig. 4*A*). However, cytoplasmic Parkin only increased at 8 h with PRO above ALC-
300 CHO (P<0.05; Fig. 4*B*). Another mitophagy-specific protein, Bcl-2/adenovirus E1B 19 kDa-
301 interacting protein-3 (BNIP3), decreased below rest at 8 h post-exercise in ALC-CHO
302 (P<0.05; Fig. 4*C*). BNIP3 was higher than both ALC-CHO and PRO treatments with ALC-
303 PRO at 8 h post-exercise, an effect paralleled by similar temporal increases in its gene
304 expression (P<0.05; Fig. 4*D*). Given the previously mentioned reduction in "general"
305 autophagy, these findings suggest that mitophagy was also inhibited by alcohol/carbohydrate
306 coingestion post-exercise.
307

DNA Fragmentation and Apoptotic Signaling

To determine whether attenuated autophagic/mitophagic responses to ALC-CHO reflected activation of apoptotic (cell death) events, we measured fragmented DNA in cytoplasmic lysates as a marker of cellular apoptosis. DNA fragmentation increased significantly by ~185% above rest at 8 h post-exercise with ALC-CHO only ($P<0.05$; Fig. 5*A*). Detection of DNA fragmentation at 8 h in both alcohol treatments was greater than PRO ($P<0.05$). Apoptosis can be executed by caspase-dependent and -independent pathways, the latter involving poly (ADP-ribose) polymerase 1 (PARP1) triggering the mitochondria-to-nuclear translocation of apoptosis inducing factor (AIF) (64). Nuclear abundance of AIF doubled above rest during early (2 h) exercise recovery in ALC-CHO ($P<0.05$; Fig. 5*B*), but declined sharply thereafter by 8 h ($P<0.01$). Within the cytoplasm, AIF levels with ALC-PRO and PRO were greater than ALC-CHO at 8 h post-exercise ($P<0.05$; Fig. 5*C*). Full-length (~116 kDa) nuclear PARP1 decreased below resting levels by 8 h in ALC-CHO only ($P<0.05$; Fig. 5*D*). As a result, PARP1 was greater than ALC-CHO with ALC-PRO and PRO at this 8 h time point ($P<0.05$). Immunoreactive ~89 kDa bands of PARP1, reduced proteolytic targets of caspase-3, were undetectable in nuclear lysates. Furthermore, we could not detect bands for the cleaved, active (~17 kDa) caspase-3 in whole muscle homogenates. Notably, pro-caspase-3 levels were greater than ALC-CHO in response to ALC-PRO and PRO at 8 h post-exercise ($P<0.05$; Fig. 5*E*). These findings suggest that alcohol-induced DNA fragmentation was elicited by caspase-independent pathways.

Nuclear and Cytoplasmic TFEB, PGC-1α, AMPK and p53

The apoptogenic effects of alcohol led us to investigate changes in the nuclear and cytoplasmic levels of several proteins highly-sensitive to changes in cellular energy availability. Nuclear and cytoplasmic levels of transcription factor EB (TFEB), a

transcriptional regulator of autophagy, decreased below rest in ALC-CHO at 8 h post-exercise (P<0.05; Fig. 6*A, B*). Nuclear TFEB at 8 h in ALC-PRO was greater than the ALC-CHO (P<0.001) and PRO (P<0.01) conditions. Following 2 h of exercise recovery in both alcohol treatments, nuclear PPARγ-coactivator-1α (PGC-1α) doubled above rest (P<0.05; Fig. 6*C*). However, its nuclear abundance returned to basal levels by 8 h for ALC-CHO only (P<0.01). Cytoplasmic PGC-1α in ALC-PRO increased above rest and ALC-CHO at 8 h (P<0.05; Fig. 6*D*). While there were no differences in nuclear AMPKα at any time point (data not shown), cytoplasmic phospho-AMPKα^{Thr172} increased above rest at 8 h in ALC-CHO only (P<0.05; Fig 6*E*). The apoptogenic p53 increased in the nucleus above rest in ALC-PRO and PRO at 8 h post-exercise (P<0.05; Fig. 6*F*). Within cytoplasmic fractions, p53 with each alcohol treatment at 8 h increased above rest and PRO (P<0.05; Fig. 6*G*), of which the largest effect occurred for ALC-CHO (P<0.01). In addition, whole muscle p53^{Ser15} phosphorylation was highest in ALC-CHO after exercise, increasing above rest at 8 h (P<0.001) and above ALC-PRO and PRO treatments (P<0.05; Fig. 6*H*).

p53- and PGC-1α-Target Genes and Oxidative Stress

We next chose to specifically focus on select p53/PGC-1α transcriptional targets that are involved in cell fate (i.e., survival or death) responses to changes in metabolic homeostasis (50). There were differential responses of p53-target genes to post-exercise alcohol ingestion. *SCO2* (synthesis of cytochrome *c* oxidase 2) expressing a protein regulating assembly of the respiratory chain cytochrome *c* oxidase (COX) complex, increased above rest with ALC-PRO at 8 h post-exercise (P<0.05; Fig. 7*A*). *SESN*-2 is an endogenous antioxidant (6) and was also elevated at this time point with ALC-CHO compared to 2 h (P<0.05; Fig. 7*B*). *PUMA* is a pro-apoptotic gene involved in mitochondrial ROS generation (10, 34) and increased above rest in all treatments (P<0.05; Fig. 7*C*), whereby the largest effect occurred for ALC-CHO

(P<0.001). In contrast, there were no changes for the pro-apoptotic *Bax* following any exercise-nutrient stimulus (data not shown). These changes in *SESN-2* and *PUMA* suggested alcohol may have induced an increase in ROS production. We therefore determined in cytoplasmic lysates the ratio of reduced to oxidized glutathione (GSH/GSSG), a major endogenous antioxidant. However, there were no significant changes in the GSH/GSSG ratio with any exercise-nutrient stimulus (Fig. 7*D*). PGC-1α can affect its own transcription (22) and there were large increases in *PGC-1α* gene expression during exercise recovery in all treatments with the largest effect prevailing 2 h post-exercise (P<0.001; Fig. 7*E*). Mitochondrial biogenesis-related PGC-1α-target genes similarly revealed divergent responses to the experimental conditions. *Tfam* (mitochondrial transcription factor A) increased above rest at 8 h post-exercise in both alcohol treatments (P<0.05; Fig. 7*F*), whereby ALC-PRO demonstrated the largest effect (P<0.01). *NRF-1* (nuclear respiratory factor-1) increased above rest at 8 h after exercise in response to ALC-PRO alone (P<0.05; Fig. 7*G*).

Mitochondrial Proteins

Suspecting that the transcriptional induction of *SCO2*, *Tfam* and *NRF-1* reflected a mitochondrial biogenesis response to post-exercise alcohol/protein ingestion, we measured the abundance of several key proteins regulating mitochondrial function. At 8 h post-exercise with ALC-PRO, there were increases above rest in the cytoplasmic content of COX subunit IV; these changes were greater than ALC-CHO and PRO (P<0.01; Fig. 8*A*). Similarly, the respiratory chain F_1-ATP synthase complex assembly factor 1 (ATPAF1) increased above rest at 8 h post-exercise in ALC-PRO only (P<0.05; Fig. 8*B*) and this change was greater than ALC-CHO (P<0.001). ATPAF1 was also elevated in PRO above ALC-CHO between 2-8 h of exercise recovery and above ALC-PRO at 2 h only (P<0.05). Voltage-dependent anion channel-1 (VDAC1), an abundant mitochondrial regulator of substrate trafficking, was higher

than ALC-CHO and PRO treatments at 8 h post-exercise in response to ALC-PRO ($P<0.01$; Fig. 8*C*). Whole muscle levels of the mitochondrial membrane fusion protein Mitofusin-2 decreased below rest at 8 h in ALC-CHO ($P<0.05$; Fig. 8*D*). Mitofusin-2 levels in ALC-PRO and PRO were greater than ALC-CHO at 8 h post-exercise ($P<0.05$). Altogether these data suggest that high-protein availability with alcohol stimulates mitochondrial biogenesis.

DISCUSSION

This is the first study to characterize the pro-apoptotic effects of acute binge alcohol consumption in human skeletal muscle following exercise. The main finding was that alcohol coingested with carbohydrate (i.e., before and after the alcohol drinking protocol) following a single bout of strenuous concurrent exercise represses autophagy and triggers intramyocellular apoptosis as indicated by DNA fragmentation. In contrast, energy-matched protein consumption attenuated alcohol-induced apoptotic responses following exercise and was accompanied by increases in markers of mitochondrial biogenesis. This apoptotic response may have been the result of alcohol imposing an additional metabolic stress to a cellular environment already disrupted by prior exercise. However, the anabolic properties of protein that increase mitochondrial protein synthesis may lower the magnitude of apoptotic events when coingested with alcohol.

Post-exercise ingestion of alcohol and carbohydrate dysregulates autophagy

We previously demonstrated that alcohol consumption following a strenuous bout of exercise repressed maximal rates of myofibrillar protein synthesis in human skeletal muscle compared to consuming protein-only beverages during recovery (41). The observation that acute alcohol exposure failed to augment proteasome-dependent protein breakdown (62) led us to investigate whether aberrant activation of autophagy, an alternate lysosome-dependent

degradative pathway sensitive to cellular bioenergetics (52), may play a role in the post-exercise alcohol-induced repression of myofibrillar protein synthesis by degrading intracellular substrate and inducing a net negative protein balance. In contrast to one of our original hypotheses, we found that by 8 h following exercise (4 h after ingesting the final alcoholic beverage), several Atgs implicated in the biogenesis of autophagic vesicles (autophagosomes) along with the nuclear and cytoplasmic content of TFEB, a transcriptional regulator of autophagy (51), were consistently attenuated (below resting values) with alcohol and carbohydrate ingestion, but not when alcohol was consumed with protein. Corresponding gene expression (except *Atg4b*) was largely unaffected at any time point, while NEDD4, an ubiquitin ligase that can "tag" Atgs such as Beclin-1 for proteasomal degradation (45), followed the same alcohol/carbohydrate-only pattern of post-exercise decline. These findings were surprising as substantial increases in autophagy alongside a reduction in proteasomal activity have previously been observed in skeletal muscle of alcoholic cirrhosis patients (60), suggesting that chronic alcohol exposure ultimately elevates skeletal muscle autophagy for constitutive removal of damaged cellular compartments.

Alcohol metabolism is energetically expensive and produces highly-toxic intermediates such as acetaldehyde and acetate (33), the latter of which has been shown to be taken up by skeletal muscle following its release from the splanchnic region in response to an acute ethanol infusion (26). Alcohol metabolism provokes mitochondrial production of ROS that can signal for the mitophagic removal of these organelles (4). Canonical mitophagy involves PINK1 accumulating on the surface of damaged/depolarized mitochondria where it recruits and activates the ubiquitin ligase Parkin (27, 63). Ubiquitinated mitochondrial proteins are subsequently delivered to autophagosomes by the bridging protein p62, which in turn undergoes degradation itself (17). Alternatively, BNIP3 is a hypoxia-sensitive mitophagy

receptor containing an LC3-interacting motif that facilitates direct autophagosomal engulfment of mitochondria (19). We found that coingestion of alcohol and carbohydrate after exercise elicited a dysregulated mitophagic response as evidenced by parallel increases in PINK1 and p62 and a reduction in BNIP3. Given that alcohol led to the consistent reduction of Atgs, the molecular "machinery" required for autophagic digestion of mitochondria, our data suggest that post-exercise alcohol intoxication prevented the disposal of potentially damaged mitochondria. Notably, when the intensity of a given stressor (i.e., alcohol) overwhelms the protective capabilities of mitophagy, intrinsic cell death (apoptotic) pathways can be activated (36). Our findings of alcohol ingestion disrupting autophagy along with an apparent, alcohol-induced downregulation of proteasome-dependent proteolysis, led us to investigate whether induction of apoptotic processes were responsible for this degradation of signaling proteins.

Post-exercise ingestion of alcohol triggers intramyocellular apoptosis

Alcohol with carbohydrate and also alcohol with protein coingestion triggered apoptotic DNA fragmentation, as revealed by the detection of post-exercise mono- and oligonucleosomes in cytoplasmic (nuclei-free) lysates. However, the largest apoptotic response prevailed for alcohol/carbohydrate and was preceded by AIF nuclear accumulation. AIF normally resides in the mitochondrial intermembrane space (58), but upon mitochondrial outer membrane permeabilization (MOMP), AIF rapidly redistributes to the nucleus where it has been shown to elicit large-scale DNA fragmentation (14). Hyperactivity of PARP1, a DNA repair enzyme, signals to AIF to facilitate its nuclear import as an alternative to the canonical cytochrome *c*/caspase-dependent pathway of mitochondrial apoptosis (29, 64). Whether PARP1 was responsible for initially signaling to AIF is unclear, as it followed a similar pattern to AIF, decreasing sharply during late (8 h) exercise recovery with

458 alcohol/carbohydrate. In addition, DNA fragmentation was not detected until 8 h post-
459 exercise and was paralleled by increases in the cytoplasmic abundance of p53, a well-
460 characterized effector of apoptosis. p53 promotes apoptosis by transcription-dependent and –
461 independent mechanisms, the latter involving MOMP, cytochrome *c* release and caspase
462 activation (11, 16, 37). Despite increased cytoplasmic p53, precursor caspase-3 levels were
463 lowest after exercise in alcohol/carbohydrate and we were unable to detect its cleaved, active
464 fragment nor evidence for nuclear cleavage of PARP1, a major caspase-3 substrate (32);
465 these effects seemingly contrast denervation-induced apoptotic signaling in rodent skeletal
466 muscle (53, 54). Thus, our findings suggest that AIF nuclear import is the initial, caspase-
467 independent driver of post-exercise alcohol-induced apoptosis. Degradation of nuclear
468 PARP1 would also limit DNA repair capacity and its decay may have perpetuated the p53-
469 independent apoptotic response. Another consideration is that the apoptotic response we
470 observed could also affect the myonuclei of myogenic cells (i.e., satellite cells) that are
471 activated in response to vigorous exercise, thereby impairing regenerative recovery,
472 particularly from the high-mechanical demands imposed by resistance exercise contraction
473 (43).
474
475 Aberrant mitophagy signaling observed in the alcohol/carbohydrate condition raises the
476 possibility that the metabolic burden of alcohol added to an intracellular environment already
477 disrupted by contractile stress (i.e., substrate depletion, altered redox state, Ca^{2+} fluctuations
478 etc.) overwhelmed mitochondrial metabolism. In this regard, the potential ATP depletion and
479 ROS generated as a result of mitochondrial alcohol metabolism may have triggered MOMP,
480 release of AIF and initiation of apoptosis, which are well-characterized features of alcohol-
481 induced liver injury (1). In support of this hypothesis, phosphorylation of cytoplasmic
482 AMPKα^{Thr172} and downstream (whole muscle) p53^{Ser15} that reflects a response to diminished

energy availability (25) peaked with alcohol/carbohydrate ingestion. This increased p53 activity could account for the largest alcohol/carbohydrate-induced mRNA expression of *PUMA* and *SESN-2*, p53-inducible genes involved in mitochondrial ROS generation (10, 34) and scavenging (6), respectively. As a DNA damage-sensitive antioxidant, *SESN-2* may have been upregulated to quench excessive ROS and combat further tissue damage. However, we found no differences in the ratio of reduced (GSH) to oxidized (GSSG) glutathione, decreases of which reflect oxidative stress (46). Direct mitochondrial measurements of ROS such as hydrogen peroxide may be a more accurate reflection of oxidative stress in human skeletal muscle (48). Nevertheless, changes in redox state arising from alcohol metabolism could have posttranslationally modified (i.e., oxidatively degraded) intracellular signaling proteins, including precursor caspase-3, which prevents its apoptotic activity (65). Indeed, limited ATP availability facilitates AIF-driven apoptosis (15, 40). Future time course studies are required to ascertain whether ATP depletion and/or mitochondrial ROS differentially activate apoptotic signal transduction following exercise and alcoholic intoxication.

Alcohol and protein coingestion may stimulate mitochondrial biogenesis

The capacity for an increase in exogenous protein availability to prevent cellular damage (e.g., preservation of Atgs) and attenuate the magnitude of alcohol-induced apoptotic DNA fragmentation was associated with an apparent activation of mitochondrial biogenesis. PGC-1α is the transcriptional "master regulator" of mitochondrial anabolism and increased rapidly in the nucleus following exercise when alcohol was consumed, deteriorating thereafter when carbohydrate was coingested. Alcohol coingested with protein otherwise facilitated nuclear retention of PGC-1α and promoted its cytoplasmic accumulation along with raising nuclear levels of TFEB, which in addition to regulating autophagosome and lysosome abundance, is a coactivator of PGC-1α and governs mitochondrial turnover (i.e., undulations of synthesis and

breakdown) (49). Hence, because autophagy (including mitophagy) was neither up- nor downregulated with alcohol and protein coingestion, the TFEB response presumably favoured mitochondrial biogenesis. Indeed, PGC-1α-inducible genes (*NRF-1*, *Tfam*) and the p53 transcriptional target *SCO2* that promote mitochondrial anabolism (21), increased to the greatest extent when alcohol and protein were coingested. Although large *PGC-1α* mRNA responses to exercise followed for all treatments, its preferential accumulation at the protein level with alcohol/protein and resultant transcriptional response (e.g., *NRF-1* upregulation) suggests that this effect was compensatory to counter the effects of alcohol exposure, since measureable increases in PGC-1α protein and rates of mitochondrial protein synthesis typically occur 18-24 h after acute exercise (3, 7, 42). In support of this postulate, mitochondrial proteins required for ATP production (COXIV, ATPAF1) and ATP trafficking (VDAC1) all increased following exercise to the greatest extent with alcohol and protein coingestion, whereas Mitofusin-2 levels, an outer mitochondrial membrane fusion protein, were unchanged, suggesting that these nascent mitochondrial proteins may have been import-incorporated into existing organelles.

Alcohol-induced ROS production is particularly damaging to mitochondrial DNA (mtDNA) due to its close proximity to the respiratory chain, and alcohol exposure has been shown to prevent mtDNA-encoded translation of proteins encoding for subunits of respiratory complexes (12). Thus, it is tempting to speculate that alcohol and protein-induced mitochondrial biogenesis represented a homeostatic matching of ATP synthesis with ROS formation to relieve mtDNA and cellular damage, thereby lowering the overall apoptotic response (i.e., reducing oxidative damage to cellular proteins etc.). The reason(s) for exogenous protein and not carbohydrate eliciting this protective response against alcohol despite matched energy content is unknown, but could be related to branched-chain amino

533 acids (BCAAs), of which whey protein is enriched, harbouring an intrinsic capacity to induce
534 skeletal muscle mitochondrial biogenesis when mitochondrial function is impaired (13). Our
535 previous finding of attenuated myofibrillar protein synthesis with alcohol/protein coingestion
536 may have culminated from a concomitant stimulation of mitochondrial protein synthesis, in
537 turn restricting available amino acid substrate for maximal stimulation of the myofibrillar
538 fraction (41). Of note is that we previously reported lower blood alcohol levels from 6-8 h of
539 exercise recovery with alcohol/protein versus alcohol/carbohydrate (41). Although the
540 mechanism(s) of this protein-induced reduction in blood alcohol is unknown, these findings
541 suggest that protein availability reduced skeletal muscle uptake of alcohol and its metabolites
542 (e.g., acetate) thus, in part, relieving mitochondria from the burden of alcohol catabolism and
543 inevitable ROS formation. It is also unclear whether protein availability before or after
544 alcohol ingestion, or the combined effects of consuming two beverages (50 g total protein), is
545 the catalyst for attenuating alcohol-inflicted cellular damage. Nonetheless, timing and
546 distribution of exogenous protein used in the current study otherwise aligns with optimal
547 anabolic feeding strategies that elevate plasma aminoacidemia to levels likely necessary to
548 counter post-exercise alcohol-induced intramuscular toxicity (2, 41). Future studies
549 investigating rates of mitochondrial protein synthesis as well as mitochondrial respiration
550 following combined exercise- and alcohol-induced intracellular stress are required to confirm
551 this thesis.
552
553 **CONCLUSION**
554 We provide novel information showing that alcohol ingestion instigates cellular apoptosis
555 following strenuous exercise. Alcohol with exogenous protein availability appeared to
556 engender skeletal muscle with an abrupt, mitochondrial anabolic response that may have
557 combated the stress imposed by alcohol metabolism (Figure 9), an effect likely mediated by

the intrinsic anabolic properties of BCAAs enriched in the whey protein beverages. While the effects of consuming alcohol alone after exercise are currently unknown, the post-exercise feeding patterns of carbohydrate and protein employed in the present investigation are consistent with recommendations for optimal nutrition following exercise-training (8, 44). As such, our data reveal several potential mechanisms unravelling how binge drinking practices could compromise sports- and exercise-training recovery-adaptation (5).

Acknowledgements

This study was funded by an ACU Collaborative Research Network Grant to JAH (2013000443). The authors would like to thank Dr. Andrew Garnham for his technical assistance during experimental trials and the subjects for their time and effort.

Disclosures

All authors report no conflict of interest.

REFERENCES

1. **Adachi M, and Ishii H**. Role of mitochondria in alcoholic liver injury. *Free Radic Biol Med* 32: 487-491, 2002.
2. **Areta JL, Burke LM, Ross ML, Camera DM, West DW, Broad EM, Jeacocke NA, Moore DR, Stellingwerff T, Phillips SM, Hawley JA, and Coffey VG**. Timing and distribution of protein ingestion during prolonged recovery from resistance exercise alters myofibrillar protein synthesis. *J Physiol* 591: 2319-2331, 2013.
3. **Baar K, Wende AR, Jones TE, Marison M, Nolte LA, Chen M, Kelly DP, and Holloszy JO**. Adaptations of skeletal muscle to exercise: rapid increase in the transcriptional coactivator PGC-1. *FASEB J* 16: 1879-1886, 2002.
4. **Bailey SM, Pietsch EC, and Cunningham CC**. Ethanol stimulates the production of reactive oxygen species at mitochondrial complexes I and III. *Free Radic Biol Med* 27: 891-900, 1999.
5. **Barnes MJ, Mundel T, and Stannard SR**. Post-exercise alcohol ingestion exacerbates eccentric-exercise induced losses in performance. *Eur J Appl Physiol* 108: 1009-1014, 2010.

6. **Budanov AV, Sablina AA, Feinstein E, Koonin EV, and Chumakov PM**. Regeneration of peroxiredoxins by p53-regulated sestrins, homologs of bacterial AhpD. *Science* 304: 596-600, 2004.
7. **Burd NA, Andrews RJ, West DW, Little JP, Cochran AJ, Hector AJ, Cashaback JG, Gibala MJ, Potvin JR, Baker SK, and Phillips SM**. Muscle time under tension during resistance exercise stimulates differential muscle protein sub-fractional synthetic responses in men. *J Physiol* 590: 351-362, 2012.
8. **Burke LM, Hawley JA, Wong SH, and Jeukendrup AE**. Carbohydrates for training and competition. *J Sports Sci* 29 Suppl 1: S17-27, 2011.
9. **Burke LM, and Read RS**. A study of dietary patterns of elite Australian football players. *Can J Sport Sci* 13: 15-19, 1988.
10. **Chipuk JE, Bouchier-Hayes L, Kuwana T, Newmeyer DD, and Green DR**. PUMA couples the nuclear and cytoplasmic proapoptotic function of p53. *Science* 309: 1732-1735, 2005.
11. **Chipuk JE, Kuwana T, Bouchier-Hayes L, Droin NM, Newmeyer DD, Schuler M, and Green DR**. Direct activation of Bax by p53 mediates mitochondrial membrane permeabilization and apoptosis. *Science* 303: 1010-1014, 2004.
12. **Cunningham CC, Coleman WB, and Spach PI**. The effects of chronic ethanol consumption on hepatic mitochondrial energy metabolism. *Alcohol Alcohol* 25: 127-136, 1990.
13. **D'Antona G, Ragni M, Cardile A, Tedesco L, Dossena M, Bruttini F, Caliaro F, Corsetti G, Bottinelli R, Carruba MO, Valerio A, and Nisoli E**. Branched-chain amino acid supplementation promotes survival and supports cardiac and skeletal muscle mitochondrial biogenesis in middle-aged mice. *Cell Metab* 12: 362-372, 2010.
14. **Daugas E, Nochy D, Ravagnan L, Loeffler M, Susin SA, Zamzami N, and Kroemer G**. Apoptosis-inducing factor (AIF): a ubiquitous mitochondrial oxidoreductase involved in apoptosis. *FEBS Lett* 476: 118-123, 2000.
15. **Daugas E, Susin SA, Zamzami N, Ferri KF, Irinopoulou T, Larochette N, Prevost MC, Leber B, Andrews D, Penninger J, and Kroemer G**. Mitochondrio-nuclear translocation of AIF in apoptosis and necrosis. *FASEB J* 14: 729-739, 2000.
16. **Dumont P, Leu JI, Della Pietra AC, 3rd, George DL, and Murphy M**. The codon 72 polymorphic variants of p53 have markedly different apoptotic potential. *Nat Genet* 33: 357-365, 2003.
17. **Geisler S, Holmstrom KM, Skujat D, Fiesel FC, Rothfuss OC, Kahle PJ, and Springer W**. PINK1/Parkin-mediated mitophagy is dependent on VDAC1 and p62/SQSTM1. *Nat Cell Biol* 12: 119-131, 2010.
18. **Gurtler A, Kunz N, Gomolka M, Hornhardt S, Friedl AA, McDonald K, Kohn JE, and Posch A**. Stain-Free technology as a normalization tool in Western blot analysis. *Anal Biochem* 433: 105-111, 2013.
19. **Hanna RA, Quinsay MN, Orogo AM, Giang K, Rikka S, and Gustafsson AB**. Microtubule-associated protein 1 light chain 3 (LC3) interacts with Bnip3 protein to selectively remove endoplasmic reticulum and mitochondria via autophagy. *J Biol Chem* 287: 19094-19104, 2012.
20. **Hawley JA, Burke LM, Phillips SM, and Spriet LL**. Nutritional modulation of training-induced skeletal muscle adaptations. *J Appl Physiol* 110: 834-845, 2011.
21. **Hood DA**. Invited Review: contractile activity-induced mitochondrial biogenesis in skeletal muscle. *J Appl Physiol (1985)* 90: 1137-1157, 2001.
22. **Jager S, Handschin C, St-Pierre J, and Spiegelman BM**. AMP-activated protein kinase (AMPK) action in skeletal muscle via direct phosphorylation of PGC-1alpha. *Proc Natl Acad Sci U S A* 104: 12017-12022, 2007.

640 23. **Jemiolo B, and Trappe S**. Single muscle fiber gene expression in human skeletal
641 muscle: validation of internal control with exercise. *Biochem Biophys Res Commun* 320:
642 1043-1050, 2004.
643 24. **Jokl EJ, and Blanco G**. Disrupted autophagy undermines skeletal muscle adaptation
644 and integrity. *Mamm Genome* 2016.
645 25. **Jones RG, Plas DR, Kubek S, Buzzai M, Mu J, Xu Y, Birnbaum MJ, and**
646 **Thompson CB**. AMP-activated protein kinase induces a p53-dependent metabolic
647 checkpoint. *Mol Cell* 18: 283-293, 2005.
648 26. **Jorfeldt L, and Juhlin-Dannfelt A**. The influence of ethanol on splanchnic and
649 skeletal muscle metabolism in man. *Metabolism* 27: 97-106, 1978.
650 27. **Kane LA, Lazarou M, Fogel AI, Li Y, Yamano K, Sarraf SA, Banerjee S, and**
651 **Youle RJ**. PINK1 phosphorylates ubiquitin to activate Parkin E3 ubiquitin ligase activity. *J*
652 *Cell Biol* 205: 143-153, 2014.
653 28. **Kim J, Kundu M, Viollet B, and Guan KL**. AMPK and mTOR regulate autophagy
654 through direct phosphorylation of Ulk1. *Nat Cell Biol* 13: 132-141, 2011.
655 29. **Kolthur-Seetharam U, Dantzer F, McBurney MW, de Murcia G, and Sassone-**
656 **Corsi P**. Control of AIF-mediated cell death by the functional interplay of SIRT1 and PARP-
657 1 in response to DNA damage. *Cell Cycle* 5: 873-877, 2006.
658 30. **Kumar V, Frost RA, and Lang CH**. Alcohol impairs insulin and IGF-I stimulation
659 of S6K1 but not 4E-BP1 in skeletal muscle. *Am J Physiol Endocrinol Metab* 283: E917-928,
660 2002.
661 31. **Lang CH, Frost RA, Deshpande N, Kumar V, Vary TC, Jefferson LS, and**
662 **Kimball SR**. Alcohol impairs leucine-mediated phosphorylation of 4E-BP1, S6K1, eIF4G,
663 and mTOR in skeletal muscle. *Am J Physiol Endocrinol Metab* 285: E1205-1215, 2003.
664 32. **Lazebnik YA, Kaufmann SH, Desnoyers S, Poirier GG, and Earnshaw WC**.
665 Cleavage of poly(ADP-ribose) polymerase by a proteinase with properties like ICE. *Nature*
666 371: 346-347, 1994.
667 33. **Lieber CS**. Metabolism of alcohol. *Clinics in liver disease* 9: 1-35, 2005.
668 34. **Liu Z, Lu H, Shi H, Du Y, Yu J, Gu S, Chen X, Liu KJ, and Hu CA**. PUMA
669 overexpression induces reactive oxygen species generation and proteasome-mediated
670 stathmin degradation in colorectal cancer cells. *Cancer Res* 65: 1647-1654, 2005.
671 35. **Livak KJ, and Schmittgen TD**. Analysis of relative gene expression data using real-
672 time quantitative PCR and the 2(-Delta Delta C(T)) Method. *Methods* 25: 402-408, 2001.
673 36. **Marino G, Niso-Santano M, Baehrecke EH, and Kroemer G**. Self-consumption:
674 the interplay of autophagy and apoptosis. *Nat Rev Mol Cell Biol* 15: 81-94, 2014.
675 37. **Mihara M, Erster S, Zaika A, Petrenko O, Chittenden T, Pancoska P, and Moll**
676 **UM**. p53 has a direct apoptogenic role at the mitochondria. *Mol Cell* 11: 577-590, 2003.
677 38. **Mizushima N, Yoshimori T, and Ohsumi Y**. The role of Atg proteins in
678 autophagosome formation. *Annu Rev Cell Dev Biol* 27: 107-132, 2011.
679 39. **Nicklin P, Bergman P, Zhang B, Triantafellow E, Wang H, Nyfeler B, Yang H,**
680 **Hild M, Kung C, Wilson C, Myer VE, MacKeigan JP, Porter JA, Wang YK, Cantley**
681 **LC, Finan PM, and Murphy LO**. Bidirectional transport of amino acids regulates mTOR
682 and autophagy. *Cell* 136: 521-534, 2009.
683 40. **Nicotera P, Leist M, Fava E, Berliocchi L, and Volbracht C**. Energy requirement
684 for caspase activation and neuronal cell death. *Brain Pathol* 10: 276-282, 2000.
685 41. **Parr EB, Camera DM, Areta JL, Burke LM, Phillips SM, Hawley JA, and**
686 **Coffey VG**. Alcohol ingestion impairs maximal post-exercise rates of myofibrillar protein
687 synthesis following a single bout of concurrent training. *PLoS One* 9: e88384, 2014.

42. **Perry CG, Lally J, Holloway GP, Heigenhauser GJ, Bonen A, and Spriet LL**. Repeated transient mRNA bursts precede increases in transcriptional and mitochondrial proteins during training in human skeletal muscle. *J Physiol* 588: 4795-4810, 2010.
43. **Petrella JK, Kim JS, Mayhew DL, Cross JM, and Bamman MM**. Potent myofiber hypertrophy during resistance training in humans is associated with satellite cell-mediated myonuclear addition: a cluster analysis. *J Appl Physiol (1985)* 104: 1736-1742, 2008.
44. **Phillips SM, and Van Loon LJ**. Dietary protein for athletes: from requirements to optimum adaptation. *J Sports Sci* 29 Suppl 1: S29-38, 2011.
45. **Platta HW, Abrahamsen H, Thoresen SB, and Stenmark H**. Nedd4-dependent lysine-11-linked polyubiquitination of the tumour suppressor Beclin 1. *Biochem J* 441: 399-406, 2012.
46. **Powers SK, Duarte J, Kavazis AN, and Talbert EE**. Reactive oxygen species are signalling molecules for skeletal muscle adaptation. *Exp Physiol* 95: 1-9, 2010.
47. **Qiao S, Dennis M, Song X, Vadysirisack DD, Salunke D, Nash Z, Yang Z, Liesa M, Yoshioka J, Matsuzawa S, Shirihai OS, Lee RT, Reed JC, and Ellisen LW**. A REDD1/TXNIP pro-oxidant complex regulates ATG4B activity to control stress-induced autophagy and sustain exercise capacity. *Nat Commun* 6: 7014, 2015.
48. **Sahlin K, Shabalina IG, Mattsson CM, Bakkman L, Fernstrom M, Rozhdestvenskaya Z, Enqvist JK, Nedergaard J, Ekblom B, and Tonkonogi M**. Ultraendurance exercise increases the production of reactive oxygen species in isolated mitochondria from human skeletal muscle. *J Appl Physiol (1985)* 108: 780-787, 2010.
49. **Scott I, Webster BR, Chan CK, Okonkwo JU, Han K, and Sack MN**. GCN5-like protein 1 (GCN5L1) controls mitochondrial content through coordinated regulation of mitochondrial biogenesis and mitophagy. *J Biol Chem* 289: 2864-2872, 2014.
50. **Sen N, Satija YK, and Das S**. PGC-1alpha, a key modulator of p53, promotes cell survival upon metabolic stress. *Mol Cell* 44: 621-634, 2011.
51. **Settembre C, Di Malta C, Polito VA, Garcia Arencibia M, Vetrini F, Erdin S, Erdin SU, Huynh T, Medina D, Colella P, Sardiello M, Rubinsztein DC, and Ballabio A**. TFEB links autophagy to lysosomal biogenesis. *Science* 332: 1429-1433, 2011.
52. **Singh R, and Cuervo AM**. Autophagy in the cellular energetic balance. *Cell Metab* 13: 495-504, 2011.
53. **Siu PM, and Alway SE**. Deficiency of the Bax gene attenuates denervation-induced apoptosis. *Apoptosis* 11: 967-981, 2006.
54. **Siu PM, and Alway SE**. Mitochondria-associated apoptotic signalling in denervated rat skeletal muscle. *J Physiol* 565: 309-323, 2005.
55. **Smiles WJ, Areta JL, Coffey VG, Phillips SM, Moore DR, Stellingwerff T, Burke LM, Hawley JA, and Camera DM**. Modulation of Autophagy Signaling with Resistance Exercise and Protein Ingestion Following Short-Term Energy Deficit. *Am J Physiol Regul Integr Comp Physiol* ajpregu 00413 02014, 2015.
56. **Steiner JL, and Lang CH**. Alcohol impairs skeletal muscle protein synthesis and mTOR signaling in a time-dependent manner following electrically stimulated muscle contraction. *J Appl Physiol (1985)* jap 00180 02014, 2014.
57. **Steiner JL, and Lang CH**. Alcohol intoxication following muscle contraction in mice decreases muscle protein synthesis but not mTOR signal transduction. *Alcohol Clin Exp Res* 39: 1-10, 2015.
58. **Susin SA, Lorenzo HK, Zamzami N, Marzo I, Snow BE, Brothers GM, Mangion J, Jacotot E, Costantini P, Loeffler M, Larochette N, Goodlett DR, Aebersold R, Siderovski DP, Penninger JM, and Kroemer G**. Molecular characterization of mitochondrial apoptosis-inducing factor. *Nature* 397: 441-446, 1999.

737 59. **Tanida I, and Waguri S**. Measurement of autophagy in cells and tissues. *Methods*
738 *Mol Biol* 648: 193-214, 2010.
739 60. **Thapaliya S, Runkana A, McMullen MR, Nagy LE, McDonald C, Naga Prasad**
740 **SV, and Dasarathy S**. Alcohol-induced autophagy contributes to loss in skeletal muscle
741 mass. *Autophagy* 10: 677-690, 2014.
742 61. **Vainshtein A, Desjardins EM, Armani A, Sandri M, and Hood DA**. PGC-1alpha
743 modulates denervation-induced mitophagy in skeletal muscle. *Skelet Muscle* 5: 9, 2015.
744 62. **Vary TC, Frost RA, and Lang CH**. Acute alcohol intoxication increases atrogin-1
745 and MuRF1 mRNA without increasing proteolysis in skeletal muscle. *Am J Physiol Regul*
746 *Integr Comp Physiol* 294: R1777-1789, 2008.
747 63. **Vives-Bauza C, Zhou C, Huang Y, Cui M, de Vries RL, Kim J, May J, Tocilescu**
748 **MA, Liu W, Ko HS, Magrane J, Moore DJ, Dawson VL, Grailhe R, Dawson TM, Li C,**
749 **Tieu K, and Przedborski S**. PINK1-dependent recruitment of Parkin to mitochondria in
750 mitophagy. *Proc Natl Acad Sci U S A* 107: 378-383, 2010.
751 64. **Yu SW, Wang H, Poitras MF, Coombs C, Bowers WJ, Federoff HJ, Poirier GG,**
752 **Dawson TM, and Dawson VL**. Mediation of poly(ADP-ribose) polymerase-1-dependent
753 cell death by apoptosis-inducing factor. *Science* 297: 259-263, 2002.
754 65. **Zeigler MM, Doseff AI, Galloway MF, Opalek JM, Nowicki PT, Zweier JL, Sen**
755 **CK, and Marsh CB**. Presentation of nitric oxide regulates monocyte survival through effects
756 on caspase-9 and caspase-3 activation. *J Biol Chem* 278: 12894-12902, 2003.

757

758

759

760

761

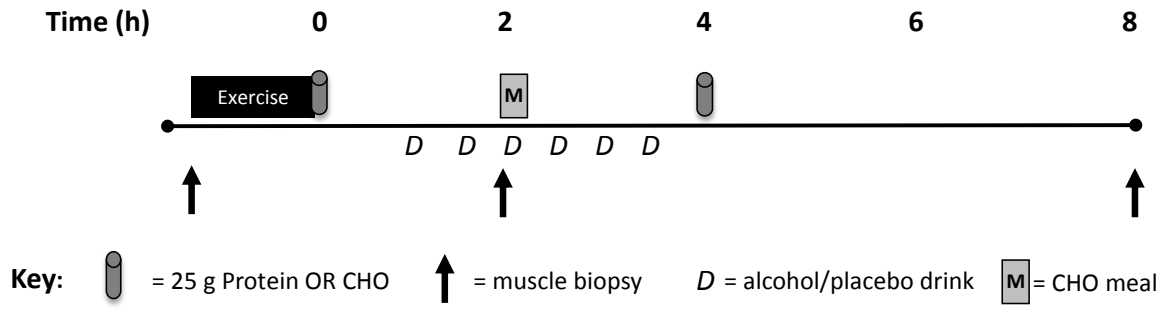

762

763

764 **Figure 1.** Schematic overview of experimental trials.

765

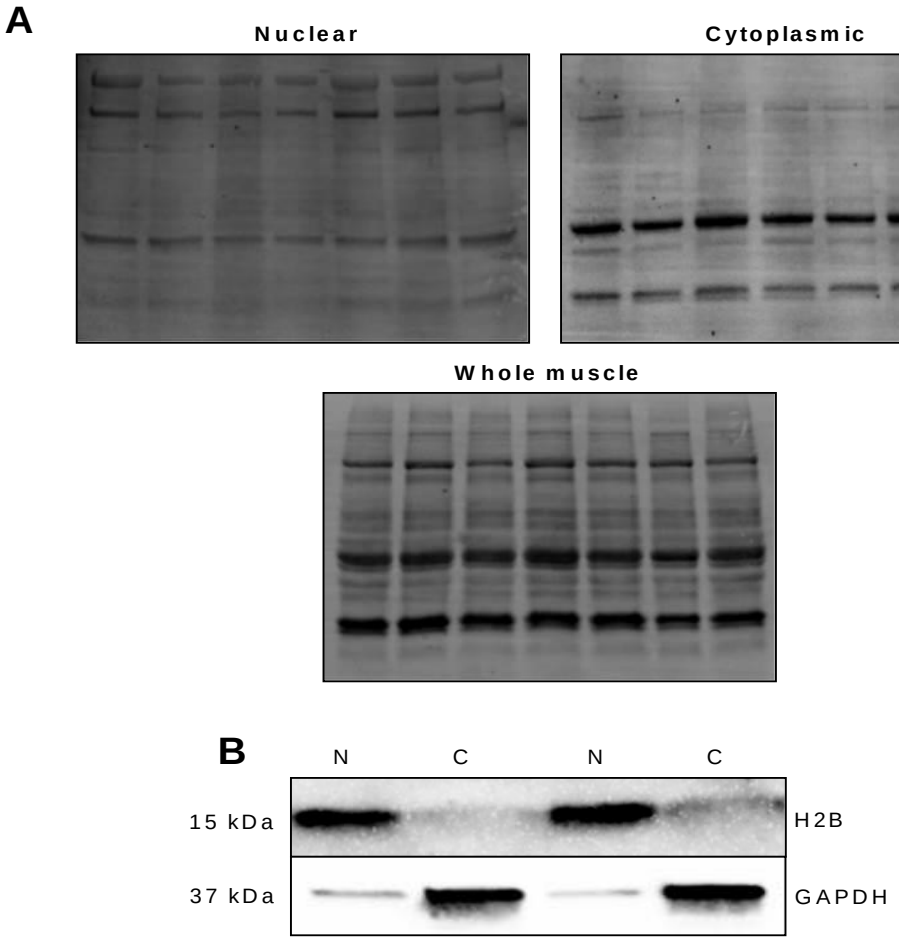

766

767 **Figure 2.** Representative Stain-Free images used for total protein normalization (*A*). Purity of

768 nuclear (N) and cytoplasmic (C) fractions were determined by immunoblotting for histone 2B

769 (H2B) and GAPDH, respectively (*B*).

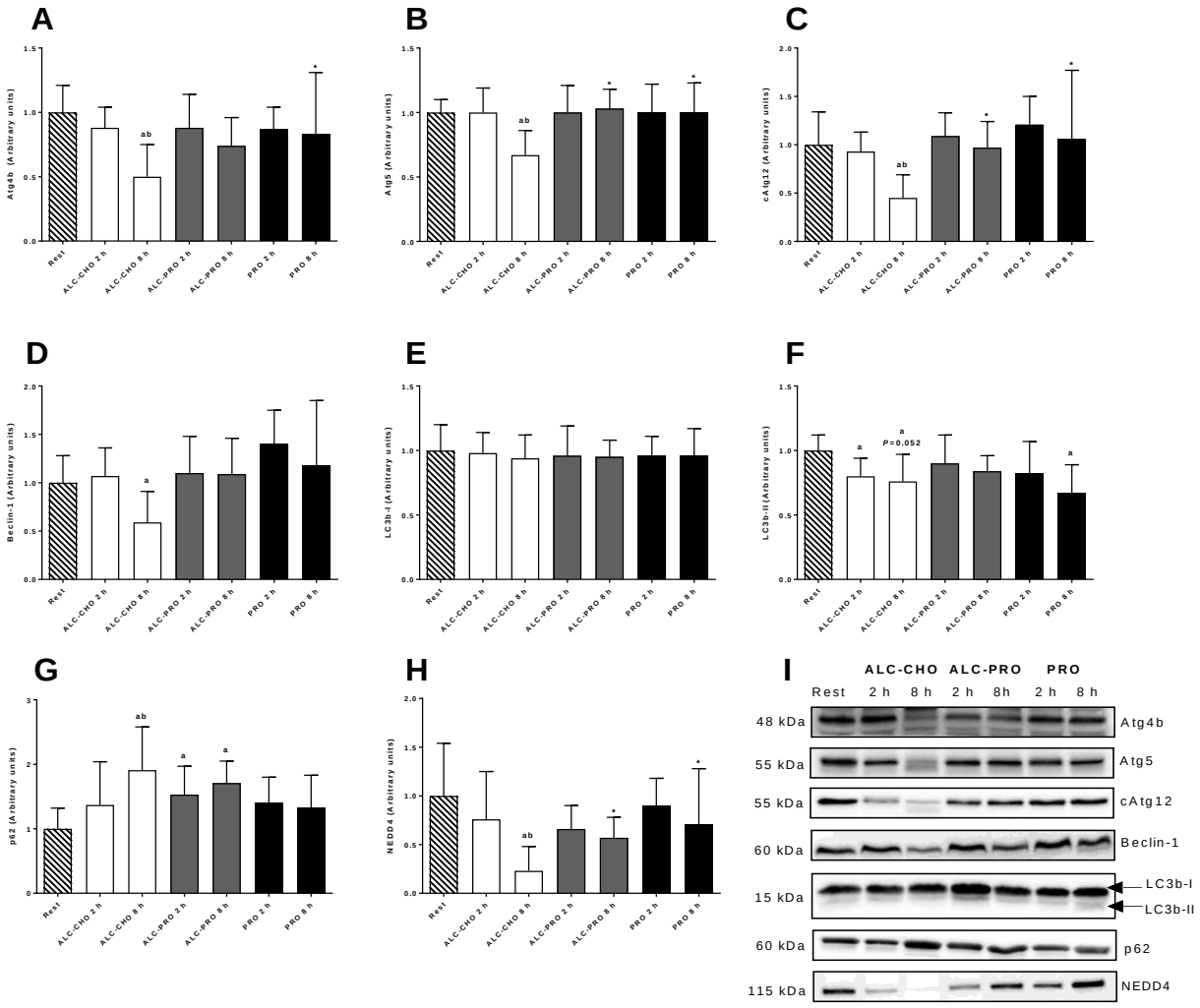

Figure 3. Whole muscle abundance of autophagy regulatory proteins Atg4b (*A*), Atg5 (*B*), cAtg12 (*C*), Beclin-1 (*D*), LC3b-I (*E*), LC3b-II (*F*), p62 (*G*), and the ubiquitin ligase NEDD4 (*n*=7 for ALC-CHO time points and ALC-PRO 2 h only; *H*) at rest and following a single bout of concurrent exercise with ingestion of either alcohol and carbohydrate (ALC-CHO), alcohol and protein (ALC-PRO), or protein only (PRO). *I*, representative images for all proteins. Data were analysed using a 2-way ANOVA with repeated measures and Student-Newman-Keuls post-hoc analysis. Values are presented (mean ± SD) as a fold change relative to resting values. Significantly different ($P<0.05$) vs. (a) rest, (b) ALC-CHO 2 h, and (*) 8 h between treatments.

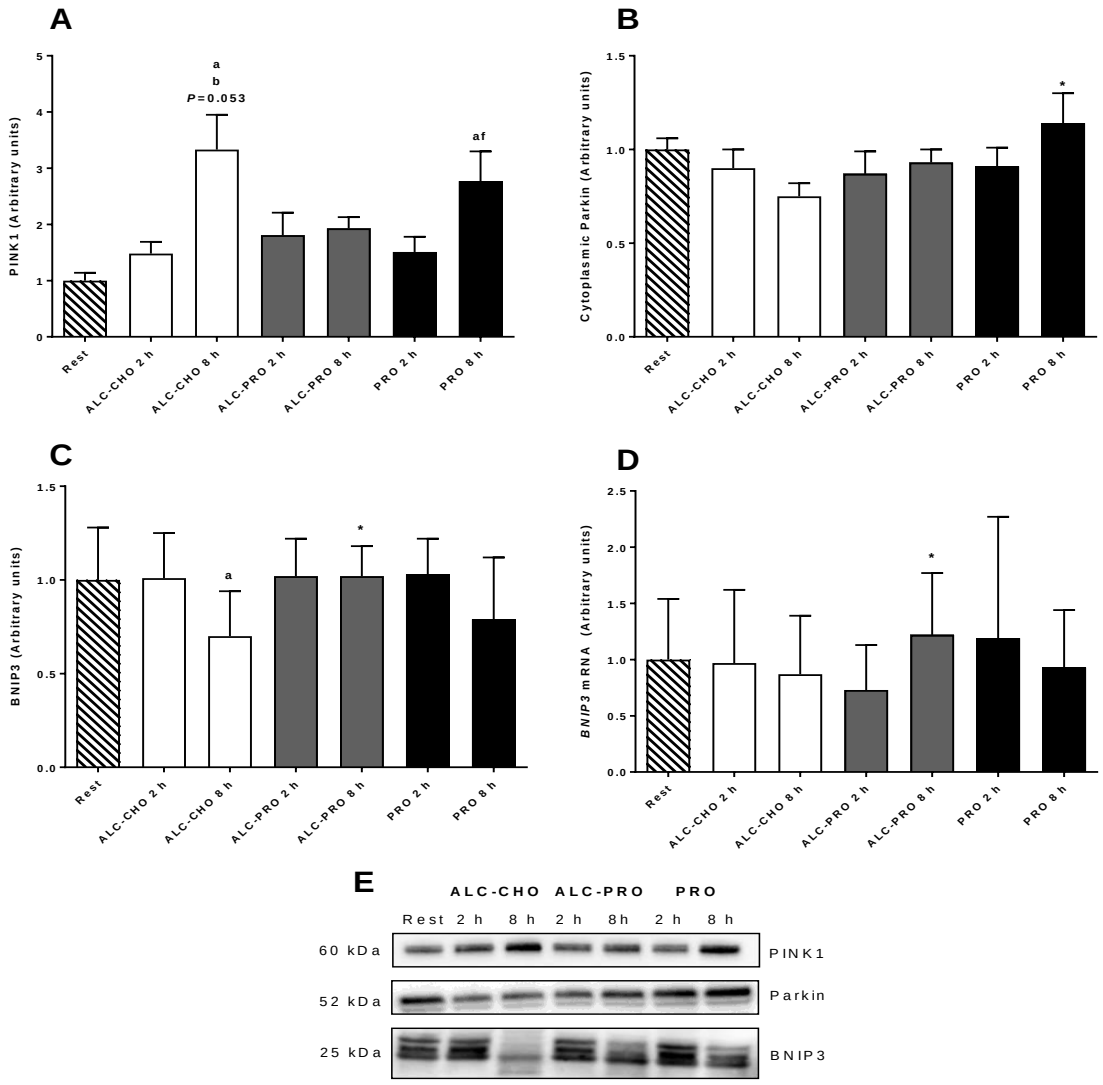

781

782 **Figure 4.** Mitophagy-related proteins PINK1 (*A*), Parkin (*B*), BNIP3 (*n*=7 for ALC-CHO 8 h
783 and ALC-PRO 2 h only; *C*), and *BNIP3* gene expression (*n*=7; *D*) at rest and following a
784 single bout of concurrent exercise with ingestion of either alcohol and carbohydrate (ALC-
785 CHO), alcohol and protein (ALC-PRO), or protein only (PRO). *E*, representative images for
786 all proteins. Data were analysed using a 2-way ANOVA with repeated measures and Student-
787 Newman-Keuls post-hoc analysis. Values are presented (mean ± SD) as a fold change
788 relative to resting values. Significantly different ($P<0.05$) vs. (a) rest, (b) ALC-CHO 2 h, (f)
789 PRO 2 h, and (*) 8 h between treatments.

790

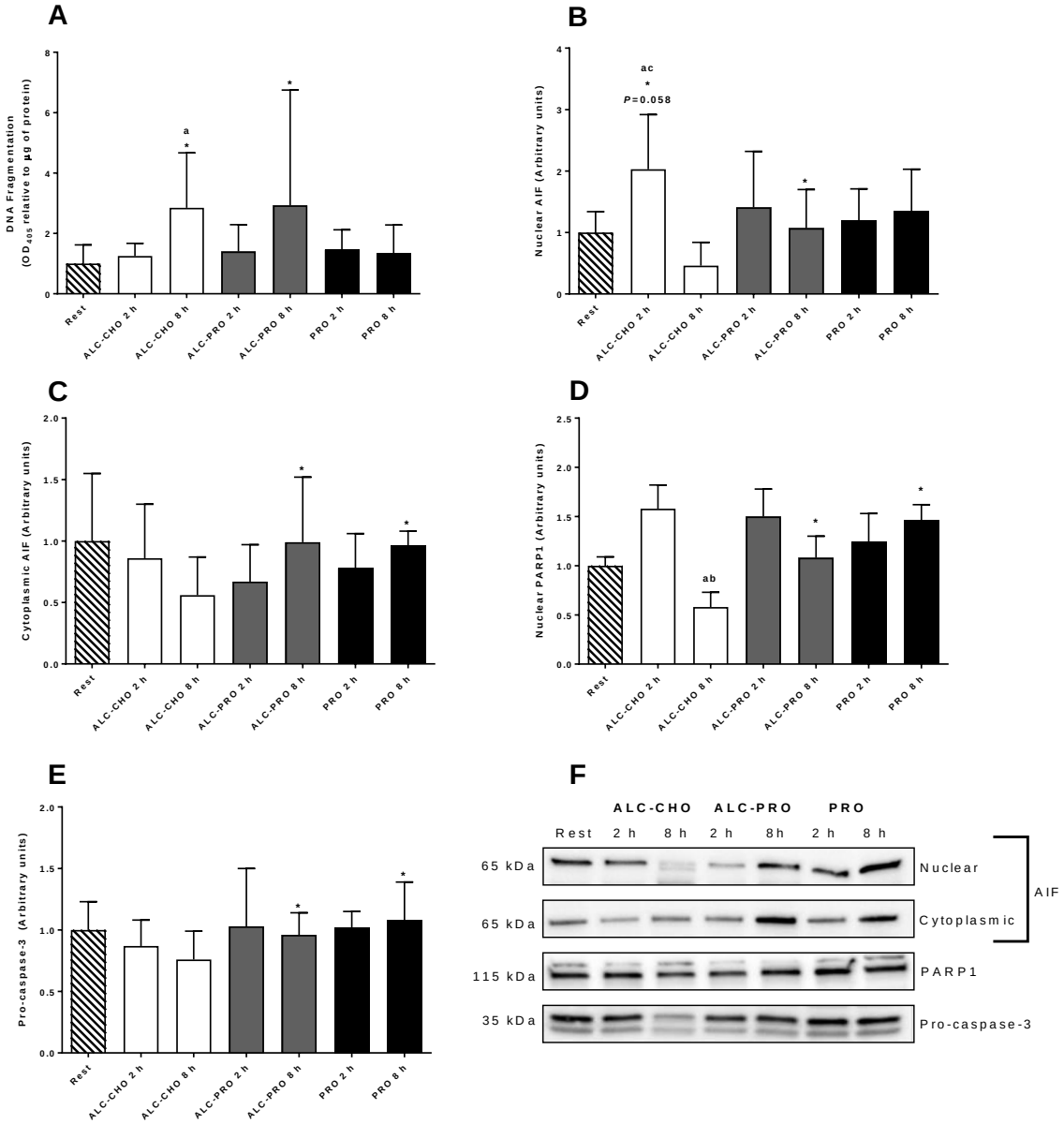

Figure 5. Apoptotic DNA fragmentation (*A*), nuclear (*B*) and cytoplasmic AIF (*C*), nuclear PARP1 (*D*), and whole muscle pro-caspase-3 (n=7 for ALC-CHO time points and ALC-PRO 2 h only; *E*) at rest and following a single bout of concurrent exercise with ingestion of either alcohol and carbohydrate (ALC-CHO), alcohol and protein (ALC-PRO), or protein only (PRO). *F*, representative images for all proteins. Data were analysed using a 2-way ANOVA with repeated measures and Student-Newman-Keuls post-hoc analysis. Values are presented (mean ± SD) as a fold change relative to resting values. Significantly different (P<0.05) vs. (a) rest, (b, c) ALC-CHO 2 and 8 h, and (*) 8 h between treatments.

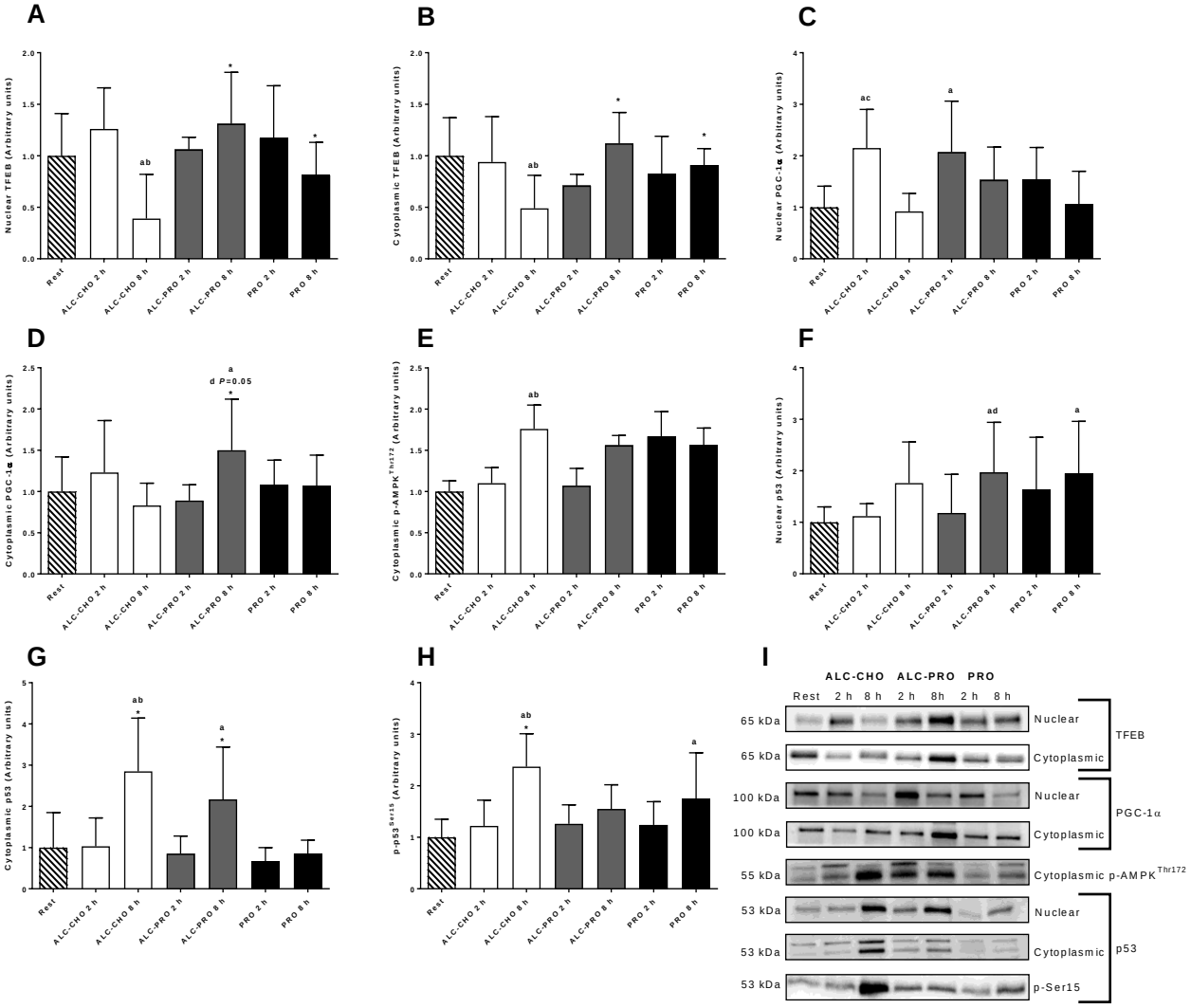

Figure 6. Nuclear (*A*) and cytoplasmic TFEB (*B*), nuclear (*C*) and cytoplasmic PGC-1α (*D*), cytoplasmic phospho-AMPKα^{Thr172} (*E*), nuclear (*F*) and cytoplasmic p53 (*G*), and whole muscle phospho-p53^{Ser15} (*H*) at rest and following a single bout of concurrent exercise with ingestion of either alcohol and carbohydrate (ALC-CHO), alcohol and protein (ALC-PRO), or protein only (PRO). *I*, representative images for all proteins. Data were analysed using a 2-way ANOVA with repeated measures and Student-Newman-Keuls post-hoc analysis. Values are presented (mean ± SD) as a fold change relative to resting values. Significantly different (P<0.05) vs. (a) rest, (b, c) ALC-CHO 2 h and 8 h, (d) ALC-PRO 2 h, and (*) 8 h between treatments.

811

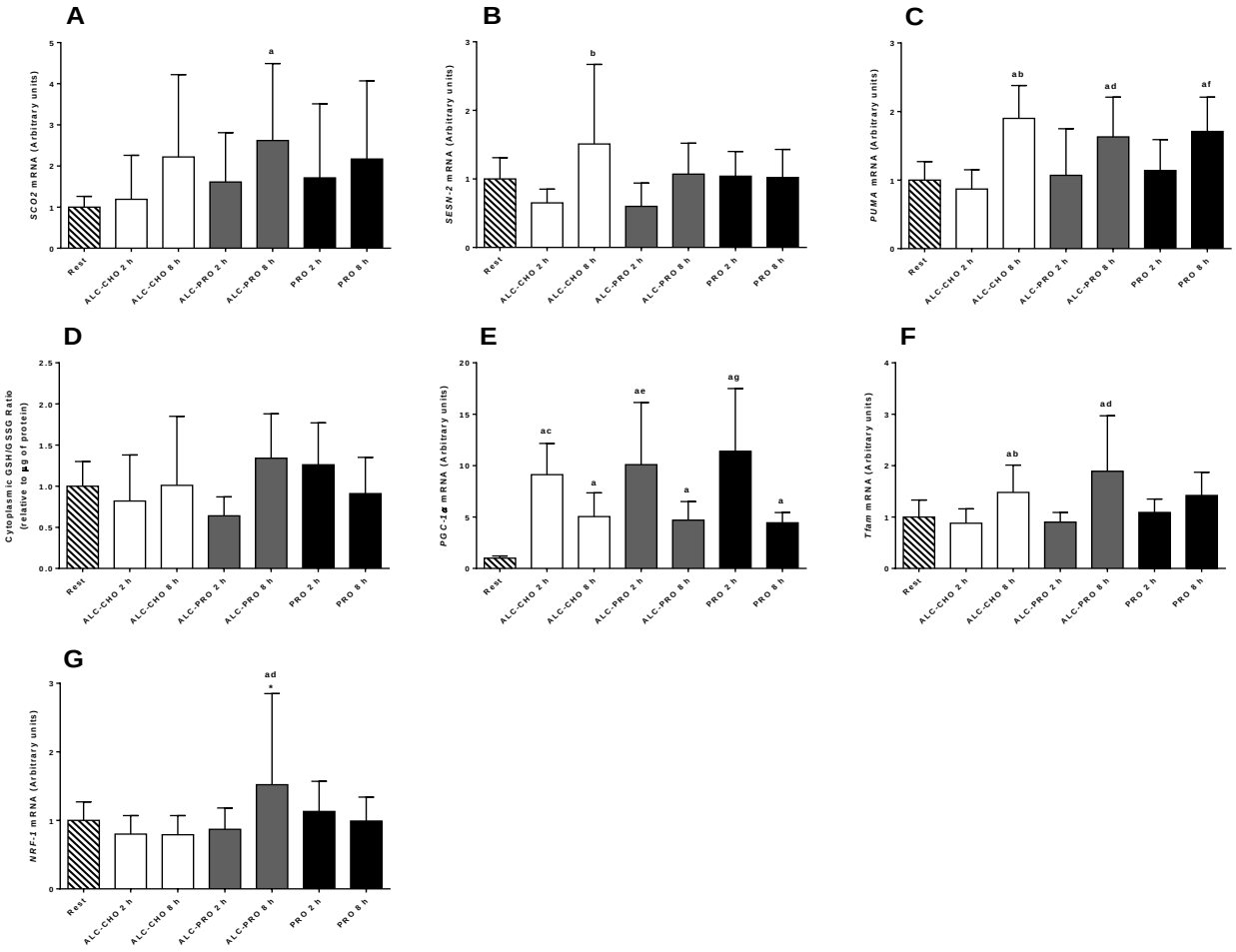

812

813 **Figure 7.** mRNA expression of *SCO2* (*A*), *SESN-2* (*B*) and *PUMA* (*C*), the cytoplasmic
814 reduced (GSH) to oxidized (GSSG) glutathione ratio (*n*=4; *D*), and *PGC-1α* (*E*), *Tfam* (*F*)
815 and *NRF-1* (*G*) mRNA at rest and following a single bout of concurrent exercise with
816 ingestion of either alcohol and carbohydrate (ALC-CHO), alcohol and protein (ALC-PRO),
817 or protein only (PRO). Data were analysed using a 2-way ANOVA with repeated measures
818 and Student-Newman-Keuls post-hoc analysis. Values are expressed relative to GAPDH and
819 presented (mean ± SD; mRNA *n*=7) as a fold change relative to resting values. Significantly
820 different ($P<0.05$) vs. (a) rest, (b, d, f) 2 h within treatments, (c, e, g) 8 h within treatments,
821 and (*) 8 h between treatments.

822

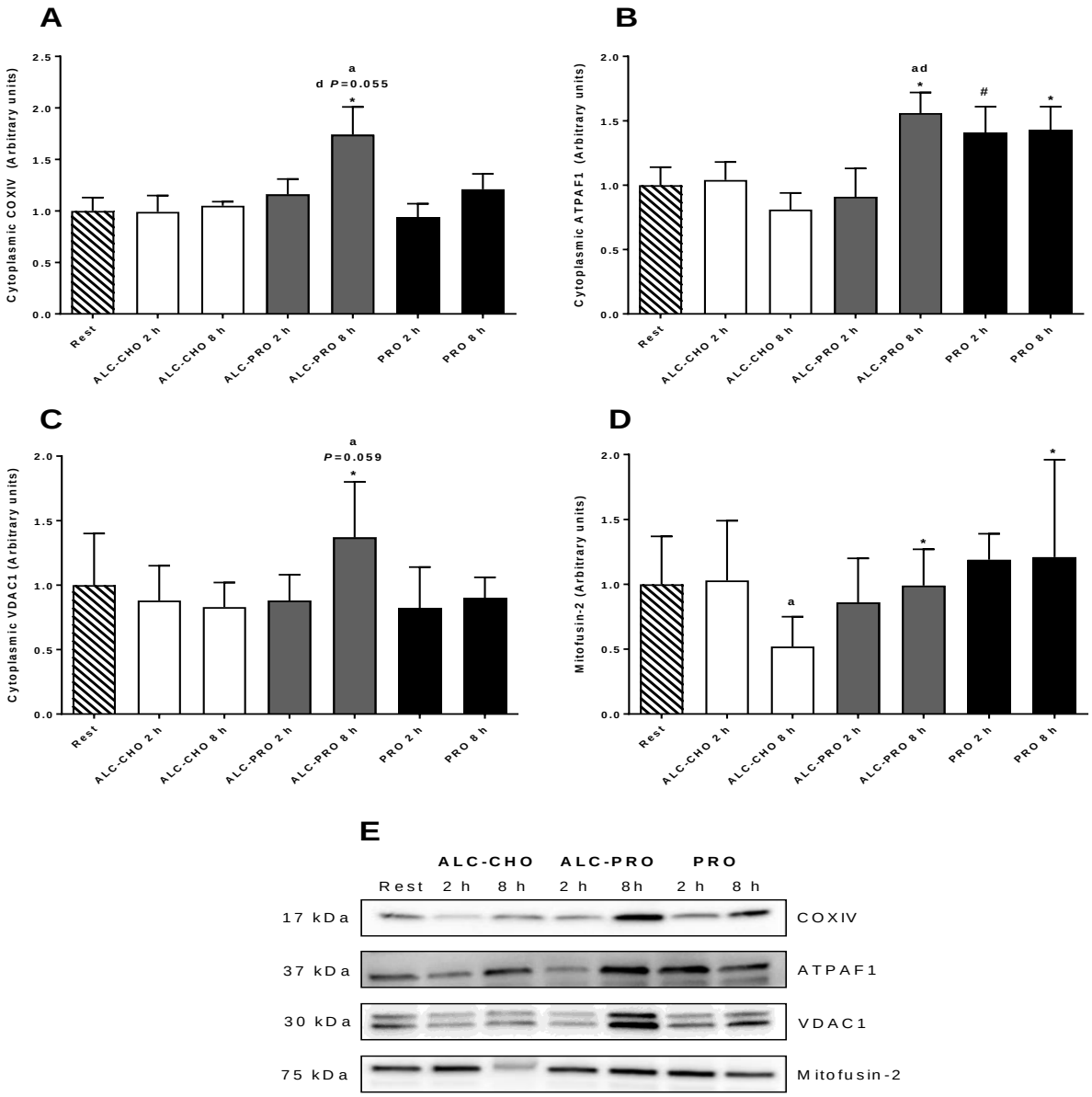

Figure 8. Cytoplasmic levels of mitochondrial proteins COXIV (*A*), ATPAF1 (*B*), VDAC1 (*C*), and whole muscle Mitofusin-2 (n=7 for ALC-CHO time points and ALC-PRO 2 h only; *D*) at rest and following a single bout of concurrent exercise with ingestion of either alcohol and carbohydrate (ALC-CHO), alcohol and protein (ALC-PRO), or protein only (PRO). *E*, representative images for all proteins. Data were analysed using a 2-way ANOVA with repeated measures and Student-Newman-Keuls post-hoc analysis. Values are presented (mean ± SD) as a fold change relative to resting values. Significantly different (P<0.05) vs. (a) rest, (d) ALC-PRO 2 h, and (#) 2 h and (*) 8 h between treatments.

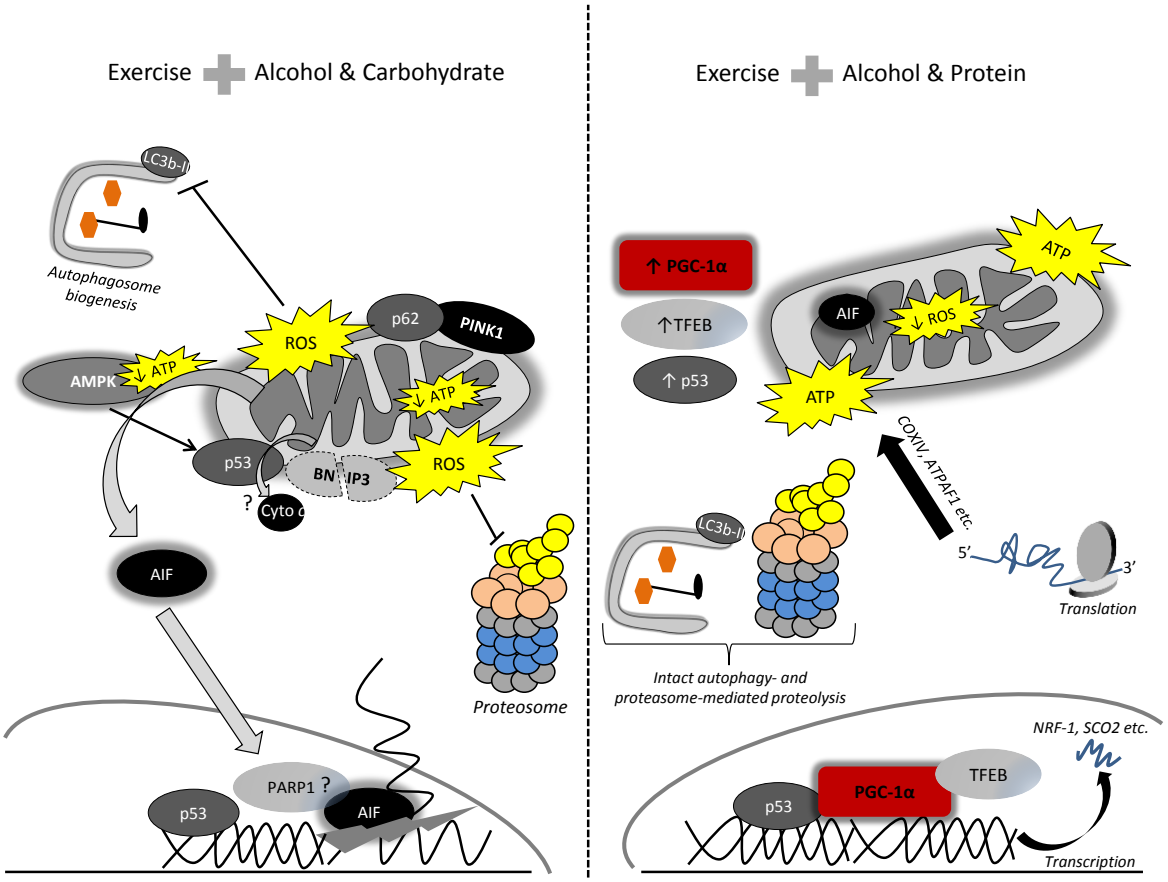

Figure 9. Hypothetical model of the effects of alcohol coingested with carbohydrate versus protein following exercise-training

Following strenuous exercise, binge alcohol consumption coingested with carbohydrate overwhelms mitochondrial respiration, leading to a reduction in cellular ATP levels and overproduction of reactive oxygen species (ROS) that causes oxidation of proteins implicated in cellular turnover (i.e., autophagy- and proteasome-mediated proteolysis). Consequently, failed clearance of damaged mitochondria, as indicated by a reduction in BNIP3 and increase in PINK1 and p62, and persistent ROS emissions could augment mitochondrial membrane permeability and trigger release of apoptogenic factors; notably, AIF (which may be recruited to the nucleus by PARP1) and cytochrome *c*, yet the latter requires confirmation. AIF nuclear translocation triggers apoptotic DNA fragmentation. In contrast, protein availability,

potentially owing to its enrichment of branched-chain amino acids, stimulates an abrupt, mitochondrial anabolic response regulated by PGC-1α, p53 and TFEB. Ultimately, the transcription of mRNA and translation of proteins integral to mitochondrial biogenesis is a homeostatic countermeasure (i.e., by increasing cellular ATP availability, attenuating ROS formation and preserving constitutive degradative pathways) to the metabolic burden imposed by alcohol introduced to an already disrupted, by prior exercise, cellular environment.